Histol Histopathol (2013) 28: 875-892
DOI: 10.14670/HH-28.875

http://www.hh.um.es

Histology and Histopathology
Cellular and Molecular Biology

Prosaposin expression in the regenerated muscles of mdx and cardiotoxin-treated mice

Cheng Li[1,4], Hui-ling Gao[1,4], Tetsuya Shimokawa[1], Hiroaki Nabeka[1], Fumihiko Hamada[1,2], Hiroaki Araki[3], Ya-ming Cao[4], Naoto Kobayashi[5] and Seiji Matsuda[1]

[1]Department of Anatomy and Embryology, [5]Medical Education Center, Ehime University Graduate School of Medicine, Toon, Ehime, Japan, [2]Department of Anatomy, Oita University Faculty of Medicine, Yuhu, Oita, Japan, [3]Division of Pharmacy, University Hospital, Toon, Ehime, Japan and [4]Department of Immunology, College of Basic Medical Sciences, China Medical University, Shenyang, China

Summary. The trophic factor prosaposin (PS) is strongly expressed in skeletal muscle, and reportedly, a PS-derived peptide attenuates loss of muscle mass after nerve injury *in vivo* and increases myoblast fusion into myotubes *in vitro*. However, few studies have focused on the role of PS during muscle regeneration. We examined the expression of PS in the skeletal muscles in normal, mdx, and cardiotoxin (CTX)-treated mice using immunofluorescence staining, Western blotting, and *in situ* hybridisation. Immunofluorescence showed intense PS immunoreactivity in the peripheral cytoplasm of uninjured myofibres of normal mice and regenerated myofibres of 8 weeks post-CTX-injection mice. In early stage CTX-treated mice (14 days and earlier), intense PS immunoreactivity was also detected in the immune cells that infiltrated damaged muscle, but it was weak for regenerating myofibres. Western blot confirmed these findings. In contrast, PS was continuously low in mdx mice in both immunofluorescence and Western blotting. *In situ* hybridisation confirmed the decrease of PS mRNA in regenerated myofibres and revealed the main form of PS mRNA as Pro+0 without a 9-base insertion both in normal and mdx mice. The embryonic myosin (MYH3) was clearly localized in the newly regenerated myofibres at 3, 7, and 14 days of post-CTX-injection and mdx mice, but was lower in the late stage of regenerated myofibres (28 and 56 days post-CTX injection). The inverse distribution of MYH3 and PS indicates that the PS expression is closely related to the differentiation of regenerated myofibres. Investigation of the mitogen-activated protein (MAP) kinase signal pathway showed the inversely synchronous correlation of phosphorylated ERK1/2 with myofibre PS and the synchronous correlation of phosphorylated p-38 with myofibre PS. These data suggest that PS is involved in the regulation of muscle differentiation of regenerated fibres.

Key words: Cardiotoxin, MAP kinase, Mdx mice, Muscle regeneration, Prosaposin

Offprint requests to: Tetsuya Shimokawa, Department of Anatomy and Embryology, Ethime University Graduate School of Medicine, Too, Ehime, Japan. e-mail: tshimo@m.ehime-u.ac.jp

Introduction

The primary functions of skeletal musculature include locomotor activity, postural behaviour, and breathing. Unfortunately, skeletal muscle is susceptible to injury after direct trauma or as a result of indirect causes such as neurological dysfunction or innate genetic defects. Trauma to skeletal muscle leads to activation of quiescent satellite cells that play an important role in muscle regeneration (Grounds et al., 2002). After muscle trauma, debris is generally removed by macrophages, which migrate into the necrotic tissue. The satellite cells are then activated and undergo differentiation into skeletal muscle precursor cells (myoblasts). These cells proliferate, fuse, and differentiate into myotubes and finally become mature muscle cells (Charge and Rudnicki, 2004). Although the degenerative and regenerative phases involved in muscle trauma and repair are similar among different muscle types and causes of injury, the kinetics and amplitude of

each phase may vary depending on the type and extent of injury and the animal model used. To study the process of muscle regeneration in a controlled and reproducible way, it has therefore been necessary to develop animal models of muscle injury.

The use of myotoxins such as cardiotoxin (CTX) is perhaps the easiest and most reproducible way to induce muscle regeneration. CTX is a peptide isolated from snake venom. It is also a protein kinase C-specific inhibitor that appears to induce the depolarisation and contraction of muscular cells, disrupt membrane organisation, and lyse various cell types (Chiou et al., 1993).

Muscle regeneration can also be studied in mouse models for muscular dystrophy. The mdx mouse strain is a mouse model for Duchenne muscular dystrophy (DMD), which is the most common lethal genetic paediatric disorder and is caused by mutations in the dystrophin gene (Bulfield et al., 1984; Attal et al., 2000). Dystrophin is part of a multi-subunit transmembrane glycoprotein complex connecting sarcolemmal proteins with the underlying skeleton and extracellular matrix. The absence of dystrophin leads to destabilisation of this complex, resulting in weaker myofibres that undergo progressive degeneration followed by massive necrosis (Tanabe et al., 1986). This is offset by a regenerative response activated by satellite cells. Regenerated fibres are morphologically typified by small-calibre, centrally nucleated fibres.

Skeletal muscle regeneration is a highly orchestrated process that involves the activation of adult muscle satellite cells to proliferate and differentiate. Satellite cell activation requires the timely, controlled upregulation of muscle transcription factors and muscle-specific genes. Various growth factors have been reported to participate in the muscle regenerative process (Charge and Rudnicki, 2004). Prosaposin (PS) was also considered to be a myotrophic factor (Rende et al., 2001). PS is a precursor of four small lysosomal proteins: saposin A, B, C, and D, which are required for intracellular degradation of certain sphingolipids (Sandhoff and Kolter, 2003). The PS gene contains 15 exons. It is transcribed into several mRNAs, resulting from alternative splicing of the 9-bp exon 8 (Holtschmidt et al., 1991). Naturally secreted PS is present in milk and in cerebrospinal and seminal fluids (Hineno et al., 1991). Various functions have been attributed to PS, mainly in the nervous and reproductive systems. It is a neurotrophic and myelinotrophic factor (O'Brien et al., 1994; Hiraiwa et al., 1999) that prevents apoptosis of neuronal cells in tissue culture (Hiraiwa et al., 1997) and acts as a neuroprotective and regenerative agent *in vivo* (Sano et al., 1994; Unuma et al., 2005; Xue et al., 2011).

To date, only a few studies have focused on the role of PS during muscle regeneration, although PS was found in the skeletal muscle over two decades ago (Sano et al., 1989; Rende et al., 2001). Rende and colleagues showed that the addition of prosaptide, a synthetic peptide derived from PS, attenuated the loss of muscle mass after nerve injury *in vivo* and increased myoblast fusion into myotubes *in vitro*. These observations are consistent with the notion that muscle cells contain and store PS and support the hypothesis of a novel myotrophic role for PS. The trophic function of PS was associated with the mitogen-activated protein kinase (MAPK) pathway (Campana et al., 1998). However, more details regarding the effects of PS on muscle regeneration are needed.

In this study we investigated the expression of PS in the skeletal muscles of mdx and CTX-treated mice. We also investigated the activity of the p38 MAPK and extracellular signal-regulated kinases 1 and 2 (ERK1/2) in gastrocnemius muscles using the same animal models.

Materials and methods

Animal models for muscle damage

Two groups of male mdx mice (C57BL/10-mdx; Clea Japan, Inc., Tokyo, Japan) aged 4 and 12 weeks, and two groups of controls (C57BL/10; Clea Japan, Inc.) of the corresponding ages were used. Three mice from each group were sacrificed and then perfused with 4% paraformaldehyde (PFA) in 0.1 M phosphate buffer (PB; pH 7.4). The skeletal muscles (including gastrocnemius, spinalis, masseter, and diaphragm) were dissected and post-fixed for 4 hours followed by haematoxylin and eosin (H&E) staining and immunofluorescence. Six mice from each group were sacrificed by decapitation and skeletal muscles were immediately dissected and stored at -80°C until used for Western blotting and *in situ* hybridisation.

C57BL/10 mice of 8-10 weeks of age were used for CTX experiments and randomly assigned to six groups (n=6). In five groups of mice, a single injection of CTX (10 μM, 50 μl, in saline) was made into the right gastrocnemius muscle. The mice were sacrificed by cervical dislocation, and the gastrocnemius muscles were dissected at 3, 7, 14, 28, or 56 days postinjection as groups 1 to 5, respectively. Saline (50 μl) was injected into the gastrocnemius of control mice, and these muscles were dissected 28 days postinjection. Following dissection, the gastrocnemius muscle of each leg was dissected into two equal parts. One part was fixed with 4% PFA and embedded in paraffin and sections were prepared for H&E staining and immunofluorescence. The other part was stored at -80°C for Western blotting (as described below).

All experiments were conducted in accordance with the Guidelines for Animal Experimentation at Ehime University School of Medicine, Japan.

Antibodies and reagents

Based on an analysis of the amino acid sequence of rat PS (M19936; Collard et al., 1988), a polyclonal antibody against rat PS was generated by immunising

rabbits with synthetic oligopeptides corresponding to the 409-PKEPAPPKQPEEPKQSALRAHVPPQK-434 proteolytic portion of PS. This sequence was obtained from an analysis of the PS amino sequence (protein secondary structure prediction, accessibility to the solvent, flexibility, surface probability, antigenecity, hydrophilicity, and dipole) and does not encode any saposins. The antiserum was affinity purified with the oligopeptide. All procedures were carried out by the Medical and Biological Laboratories Co., Ltd. (Nakaku, Nagoya, Japan). The species reactivity was also confirmed in mice by Western blotting.

The mouse monoclonal anti-myosin (skeletal, fast) antibody was purchased from Sigma-Aldrich (St Louis, MO, USA), and the mouse monoclonal anti-CD68 antibody that recognises mononuclear cells (especially macrophages) was from Thermo Fisher Scientific (Fremont, CA, USA). The goat anti-MYH3 (myosin heavy chain 3, also known as muscle embryonic myosin heavy chain) was from Santa Cruz Biotechnology, Inc. (Santa Cruz, CA, USA), and the anti-GAPDH antibody was purchased from Imgenex (San Diego, CA, USA). Rabbit anti-phospho-ERK1/2 (Thr202/Tyr204), rabbit anti-ERK1/2, rabbit anti-phospho-p38 (Tyr182), and rabbit anti-p38 were purchased from EnoGene Biotech (New York, NY, USA). Horseradish peroxidase (HRP)-conjugated anti-rabbit IgG was acquired from KDL (Gaithersburg, MD, USA). Avidin-conjugated fluorochrome (Avidin-Alexa 488), donkey anti-goat Alexa 488, and goat anti-rabbit-Alexa 546 antibodies were purchased from Invitrogen (Carlsbad, CA, USA).

CTX from *Naja mossambica* was purchased from Sigma-Aldrich, the M.O.M. kit was acquired from Vector Laboratories (Burlingame, CA, USA), the DC Protein Assay Kit was obtained from Bio-Rad (Hercules, CA, USA), and the enhanced chemiluminescence (ECL) system was purchased from GE Healthcare (Piscataway, NJ, USA). NBT-2 emulsion and D-19 developer were obtained from Kodak (Rochester, NY, USA).

H&E staining and nuclei assessments

The gastrocnemius muscles from CTX-treated mice and the skeletal muscles (gastrocnemius, spinalis, masseter, and diaphragm) from mdx and control mice were fixed and dehydrated using a graded ethanol series, cleared in xylene, embedded in paraffin and sectioned at a thickness of 7 μm. Sections were prepared and stained routinely with H&E and examined under a photomicroscope (E800M; Nikon, Tokyo, Japan).

Six sections from each mdx and C57BL/10 mouse of 4 and 12 weeks (n=3 in each group) were assessed for percentage of fibres with internal nuclei. On average, 1 000 fibres were counted per section. Representative sections were photographed using a digital camera system (Digital Sight DS-Fi1; Nikon). The percentage of fibres containing central nuclei derived from each of the experimental groups was statistically compared with the control groups.

Immunofluorescence staining

Paraffin blocks containing skeletal muscles of CTX-treated, mdx, and control mice were prepared as described using H&E staining. The 7-μm-thick paraffin sections were dewaxed in 100% xylene, put through an ethanol rehydration series, and finally washed with distilled water then transferred to phosphate-buffered saline (PBS). The slides were then pretreated with Liberate Antibody Binding Solution (Polysciences, Inc., Warrington, PA, USA) for 5 minutes at room temperature to expose epitopes for staining. Following a brief wash in PBS, slides were blocked in M.O.M. mouse IgG blocking reagent for 1 hour at room temperature, rinsed, and incubated for 5 minutes in the M.O.M. diluent solution. The slides were then incubated overnight at 4°C in M.O.M. diluent solution containing mouse monoclonal anti-skeletal myosin (or mouse monoclonal anti-CD68, 1:100 dilution) and rabbit anti-PS-Ab (1:100 dilution). Following washing with PBS, the sections were treated with a working solution of M.O.M. containing biotinylated anti-mouse IgG reagent (1:250) for 1 hour at room temperature and washed with PBS. The sections were then treated with avidin-conjugated fluorochrome (Avidin-Alexa 488) and anti-rabbit-Alexa 546 (both 1:400) in blocking solution for 2 hours at room temperature and treated with DAPI (1:1000) for 10 minutes.

For anti-MYH3, sections were incubated in blocking solution (5% BSA/0.1% gelatin/0.1% Triton X-100 in PBS) for 1 hour at room temperature and then with primary antibodies (goat anti-MYH3 and rabbit anti-PS-Ab, both 1:100 dilution) at 4°C overnight. Following washing with PBS, the sections were treated with donkey anti-goat Alexa 488 and goat anti-rabbit Alexa 546 (both 1:400) in blocking solution for 2 hours at room temperature followed by DAPI (1:1000) for 10 minutes.

The sections were then washed with PBS, mounted, and examined under a confocal fluorescence microscope (A1; Nikon). The tissues were analysed at 20x and 60x.

Western blotting

The gastrocnemius muscles from CTX-treated mice and the skeletal muscles (gastrocnemius, spinalis, masseter, and diaphragm) from mdx and control mice were homogenised in ice-cold lysis buffer containing 50 mM Tris (pH 7.5), 150 mM NaCl, 1 mM ethylene-diaminetetraacetic acid (EDTA), 0.1% sodium dodecyl sulfate (SDS), 0.25% sodium deoxycholate, 1% NP-40, and 2 mM NaVO3 with protease inhibitor and phosphatase inhibitor cocktails. A total protein extract of each of the skeletal muscles was heated at 96°C for 5 minutes and pelleted by centrifugation at 12000xg. Protein concentrations were determined with a DC Protein Assay. Equal amounts of tissue extract protein (30 μg) were loaded into each lane and run in parallel with pre-stained molecular weight markers (Bio-Rad) in

10% SDS-polyacrylamide gel electrophoresis (PAGE) before being transferred to a polyvinylidene difluoride membrane (Millipore, Bedford, MA, USA). After blocking, the membrane was immunolabelled with rabbit anti-PS-Ab, anti-phospho-ERK1/2, anti-ERK1/2, anti-phospho-p38, anti-p38 (1:400), and rabbit anti-GAPDH (1:1000). The immunoreaction was visualised with HRP-conjugated anti-rabbit immunoglobulin (1:2000) and ECL (using ECL plus substrate solution) and either exposed to X-ray films (RX-U; Fuji, Tokyo, Japan) or detected with Image Quant LAS 4000 (GE Healthcare). Band intensity was analysed using Quantity One software (version 4.6.2; Bio-Rad).

In situ hybridisation

Mdx and C57BL/10 mice of 4 and 12 weeks were sacrificed by decapitation. The skeletal muscles were immediately dissected and frozen on dry ice, then stored at -80°C. Sections were cut on a cryostat (20 μm thick), thaw-mounted onto silane-coated slides and stored at -80°C until use.

Three antisense 36-mer oligonucleotide probes, AS1, AS3, and AS4, and one sense probe, SS1 (used for control), were synthesised commercially (Operon Biotechnologies, Inc., Tokyo, Japan). AS1 was complementary to bases 1704 to 1739 in the 3'-untranslated region of PS cDNA, permitting the detection of total PS mRNA. AS3 was synthesised to detect Pro+9 mRNA (exon 8-containing PS mRNA), as the sequence of the PS cDNA determined by Collard et al. (1988) contained the 9-base insertion after base 801 of PS cDNA (Hiraiwa et al., 2003). In contrast, AS4 was complementary to bases 778 to 813 of PS cDNA, which excludes the 9-base insertion and thus detects Pro+0 mRNA (exon 8-excluded PS mRNA). As a control, the sense probe SS1 was complementary to AS1. The sequences of the four probes were as follows:

AS1: 5'-TTCATTACCCTAGACCCACAAGTAG GCGACTTCTGC-3'

SS1: 5'-GCAGAAGTCGCCTACTTGTGGGTCT AGGGTAATGAA -3'

AS3: 5'-CTTGGGTTG*CTGATCCTG*CATGTGC ATCATCATCTG-3'

AS4: 5'-TTCCTTGGGTTGCATGTGCATCATCA TCTGGACGGC-3'.

The sequence in italics (AS3) is complementary to the 9-base insertion. The underlined sequences in AS3 and AS4 are the shared sequences. The probes were labelled with [^{35}S]dATP (46.2 TBq/mmol; PerkinElmer Life Sciences, Boston, MA, USA) by terminal deoxynucleotidyl transferase (Takara, Tokyo, Japan), and a specific activity of approximately 1.0×10^7 dpm/ml was obtained.

In situ hybridisation was performed as previously described (Chen et al., 2008). Briefly, sections were fixed in 4% PFA in 0.1 M sodium PB (pH 7.4) for 15 minutes, rinsed in 4x standard saline citrate (SSC, pH 7.4) and dehydrated through a graded ethanol series. Sections were then hybridised with ^{35}S-labelled probes in hybridisation buffer (50% deionised formamide, 1% Denhardt's solution, 250 μg/ml yeast total RNA, 0.1 g/ml dextran sulphate, 0.12 M PB, 20 mM DTT in 4x SSC) at 41°C overnight. After hybridisation, sections were rinsed three times in 1xSSC at 55°C for 20 minutes, dehydrated through a graded ethanol series, coated with Kodak NBT-2 emulsion, and exposed at 4°C for 4 weeks. Finally, the sections were developed in a D-19 developer and counterstained with H&E. Following dehydration and mounting, the sections were observed under a microscope. The positive and total cells were counted according to the density of silver grains in nuclei (Simerly et al., 1990).

Statistics

Data are given as the mean±standard error of the mean (SEM). Statistical analyses were performed using a Mann-Whitney U-test between two groups. An analysis of variance (ANOVA) followed by Fisher's least significant difference (LSD) *post hoc* tests were used to analyse three or more groups. All analyses were performed using SPSS 16.0 (SPSS Inc., Chicago, IL, USA). $p<0.05$ and $p<0.01$ were considered to indicate statistical significance.

Results

PS expression in regenerated myofibres injured by cardiotoxin

To assess the role of PS in muscle regeneration, we chose to conduct the studies in CTX-induced muscle injury. Muscle regeneration in gastrocnemius muscle was induced by direct injection of CTX and induced extensive and reproducible muscle necrotic injury. H&E staining documented that myogenic differentiation was initiated within 3 days following CTX injection. Newly regenerated myotubes with central nuclei were observed on day 3, together with a great number of infiltrating or inflammatory cells accumulated in the injured muscles (Fig. 1b). The numbers of infiltrating cells and necrotic fibres were greatly reduced, and regenerating muscle fibres with central nuclei became considerably larger on day 7 (Fig. 1c). Muscle architecture was largely restored 14 days after muscle injury (Fig. 1d-f).

Immunofluorescence was performed to analyse the expression of PS in gastrocnemius muscles (Fig. 1g-r). Myosin (fast) was used as a muscle marker, best known for its role in muscle contraction and involvement in a wide range of eukaryotic motility processes. PS immunoreactivity in the gastrocnemius muscle of control mice was distributed in the peripheral cytoplasm (Fig. 1m). PS immunoreactivity was evident in non-muscle infiltrating cells on day 3 and day 7 post-CTX injection (shown as arrowheads in Fig. 1n,o). The infiltrating cells were confirmed as macrophages with anti-CD68 (Fig. 2). When muscle architecture was restored, PS

immunoreactivity in the regenerated muscle was low, with an obvious decrease in infiltrating cells on days 14 and 28 post-CTX injection (Fig. 1p,q). On day 56, immunoreactivity was recovered (arrows in Fig. 1r).

Embryonic myosin heavy chain (MYH3) expression was examined as a marker of muscle regeneration (Whalen et al., 1990) 3, 7, 14, 28, and 56 days after CTX injection (Fig. 3). MYH3 immunoreactivity was evident in newly regenerated myofibres on days 3, 7 and, 14 post-CTX injection (Fig. 3b-d). When muscle architecture was restored, MYH3 immunoreactivity in the regenerated muscle became low after day 28 post-CTX injection (Fig. 3e, f).

We confirmed localisation variations of PS protein levels in the gastrocnemius muscle by Western blotting (Fig. 4). Compared with control mice, PS protein levels were greatly elevated in post-CTX-treated muscles on day 3 ($p<0.05$). The increased levels of PS coincided with muscle regeneration. On day 7 after CTX injection, PS protein levels were no different from those of the control, while on day 14, PS levels were significantly lower ($p<0.05$ vs. control group). The PS level recovered from day 28. As an internal standard, no significant change in GAPDH levels was noted among the different groups.

Histopathological examination of young and adult mdx mice muscle

H&E staining was performed using the skeletal muscles of the mdx and control mice and the result of the gastrocnemius was shown in Figure 5. In mdx mice, regenerated myofibres were identified co-existing with normal myofibres at 4 weeks of age (Fig. 5b); with most myofibres replaced by regenerated myofibres with varying fibre diameters at 12 weeks of age (Fig. 5d). In the control group, almost no regenerated myofibres with central nuclei were observed at either time point (Fig. 5a,c). The increasing proportion of regenerated fibres with central nuclei was apparent in mdx muscles of both 4 and 12 weeks compared with age-matched controls (Fig. 5e). Additionally, the percentage observed in mdx muscle was higher at 12 than at 4 weeks (59.02±7.24% vs. 27.34±9.20%, respectively; $p<0.01$), consistent with previous reports (Torres and Duchen, 1987). The results for the other skeletal muscles were similar to the gastrocnemius (data not shown).

PS expression in young and adult mdx mice

To clarify the localisation of PS in the skeletal

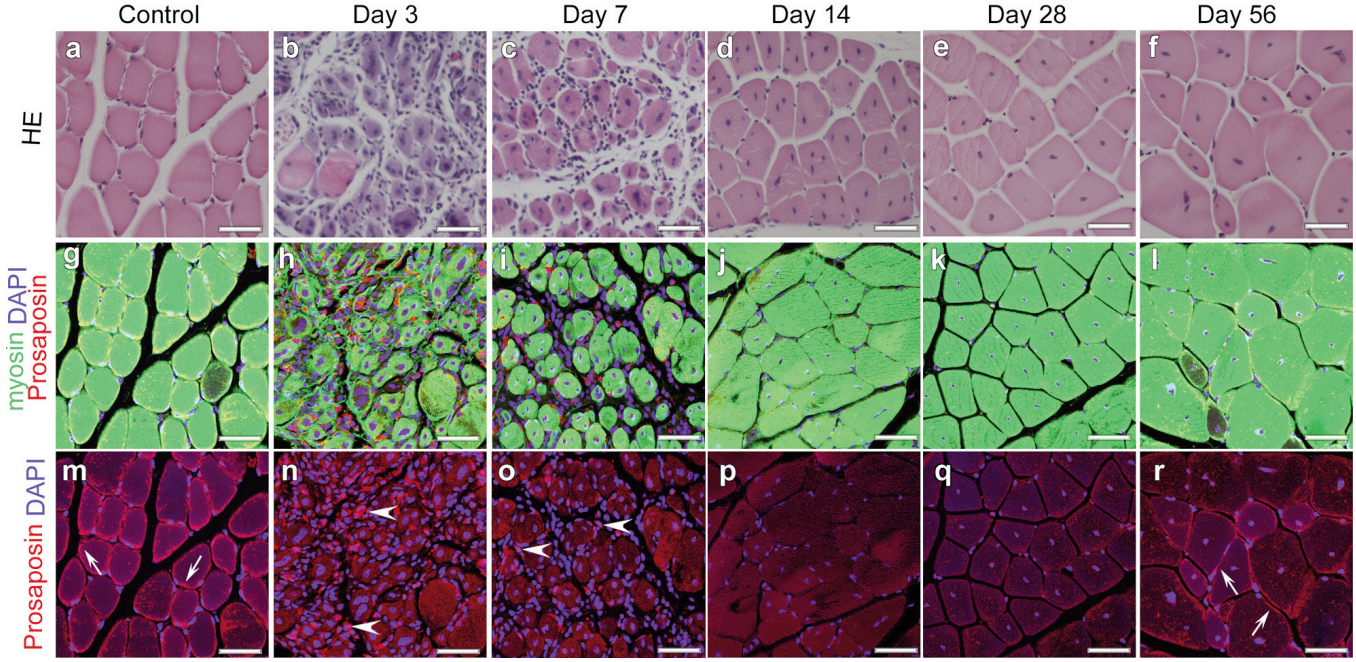

Fig. 1. Impaired skeletal muscle regeneration and PS immunoreactivity in gastrocnemius muscles of C57BL/10 mice. Paraffin sections were subjected to H&E staining **(a-f)** and immunofluorescence **(g-r)** 3, 7, 14, 28, and 56 days after CTX injection. Saline was injected into the gastrocnemius of control mice. Immunofluorescence results for myosin, a marker for myofibres, are shown in green. Nuclei stained by DAPI are in blue. Prosaposin is shown in red. Arrows **(m, r)** indicate the PS immunoreactivity in the peripheral cytoplasm of myofibres. The arrowheads **(n, o)** indicate the infiltrating cells with PS immunoreactivity. Bars: 20 μm.

muscles of C57BL/10 and mdx mice, immunofluorescence staining of PS with myosin was conducted on tissue samples (Fig. 6). The PS immunoreactivity in the gastrocnemius muscles of C57BL mice was distributed in the peripheral cytoplasm in mice at 4 (Fig. 6a-d) and 12 weeks (Fig. 6k-n). In contrast, PS immunoreactivity in regenerating muscles in mdx mice was much weaker (asterisks in Fig. 6e-j, o-r). However, PS immunoreactivity was distributed in some non-muscle cells of mdx mice (arrowheads in Fig. 6g,p).

To identify the type of non-muscle cells, immunofluorescent staining of CD68 with PS was conducted using gastrocnemius sections from 12-week mdx mice. The co-localisation of PS with CD68 in these cells (arrows in Fig. 7) indicates that the non-muscle cells in mdx were macrophages.

Western blot analysis was performed to investigate and compare the expression of PS protein in mdx and C57BL/10 mice at 4 (Fig. 8a, c) and 12 weeks (Fig. 8b, d). Because the anti-PS antibody was obtained from the intermediate sequence between saposin C and D, it only reacts with PS rather than with saposins. PS band intensity was analysed using Quantity One software. Mann-Whitney U-tests revealed significant decreases compared with the control in PS expression levels detected in mdx gastrocnemius muscles in mice at both 4

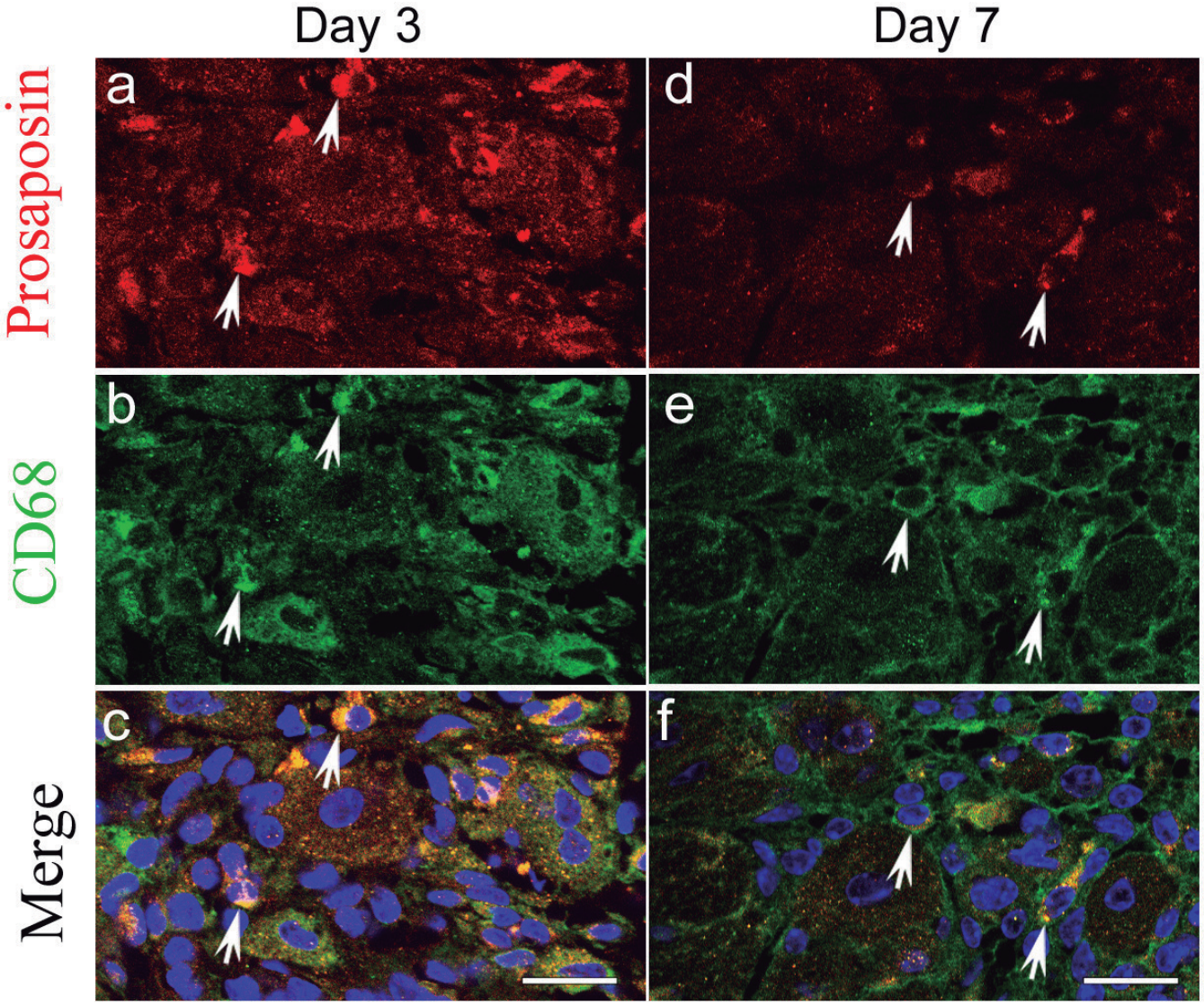

Fig. 2. PS localization in the CD68-positive cells in CTX-treated gastrocnemius muscle 3 and 7 days after CTX injection. Immunofluorescence staining of PS (red) and CD68 (green) in the gastrocnemius muscle. DAPI stained the nuclei blue. Arrows indicate that PS co-localised with CD68 in the cytoplasm of inflammatory cells. CD68 is a marker for mononuclear cells. Bars: 20 μm.

and 12 weeks (Fig. 8c, d; $p<0.01$). The decrease was more obvious in 12-week than in 4-week mdx mice (0.55 ± 0.11 vs. 0.68 ± 0.11; $p<0.01$).

We additionally investigated other muscle types (masseter, spinalis, and diaphragm). Although the study on the morphological aspects showed different degrees of deterioration among the gastrocnemius, diaphragm, and masseter (Muller et al., 2001), the expression pattern of PS was similar in these muscles in our study. The expression of PS was lower in both 4-week and 12-week mice compared with control mice (data not shown).

Immunofluorescent staining of MYH3 with PS was conducted using gastrocnemius sections from 4- and 12-week control and mdx mice. MYH3 was clearly localised in the cytoplasm of regenerated myofibres in 4-week and 12-week mdx mice but was less so in the control muscles (Fig. 9).

PS mRNA expression

We analysed the expression of PS mRNA in the skeletal muscles of mdx mice at 4 weeks of age. Regenerated myofibres were characterised by central nuclei that regularly aligned in longitudinal sections (Fig. 10).

Two alternative splicing forms exist for PS mRNA: Pro+9 and Pro+0. In the C57BL mice gastrocnemius muscle, the hybridization signals of total mRNA (AS1) and Pro+0 (AS4) were strongly expressed (Fig. 10e,f,n,o), whereas Pro+9 (AS3) was weak (Fig. 10j,k). These findings indicate that the main isoform in the myoblasts and myotubes were Pro+0. In the mdx, AS1 and AS4 (Fig. 10g,i,p,q) were also stronger than AS3 but weaker than those of the C57BL muscles (Fig. 10e,f,n,o). Similar results were obtained at 12 weeks

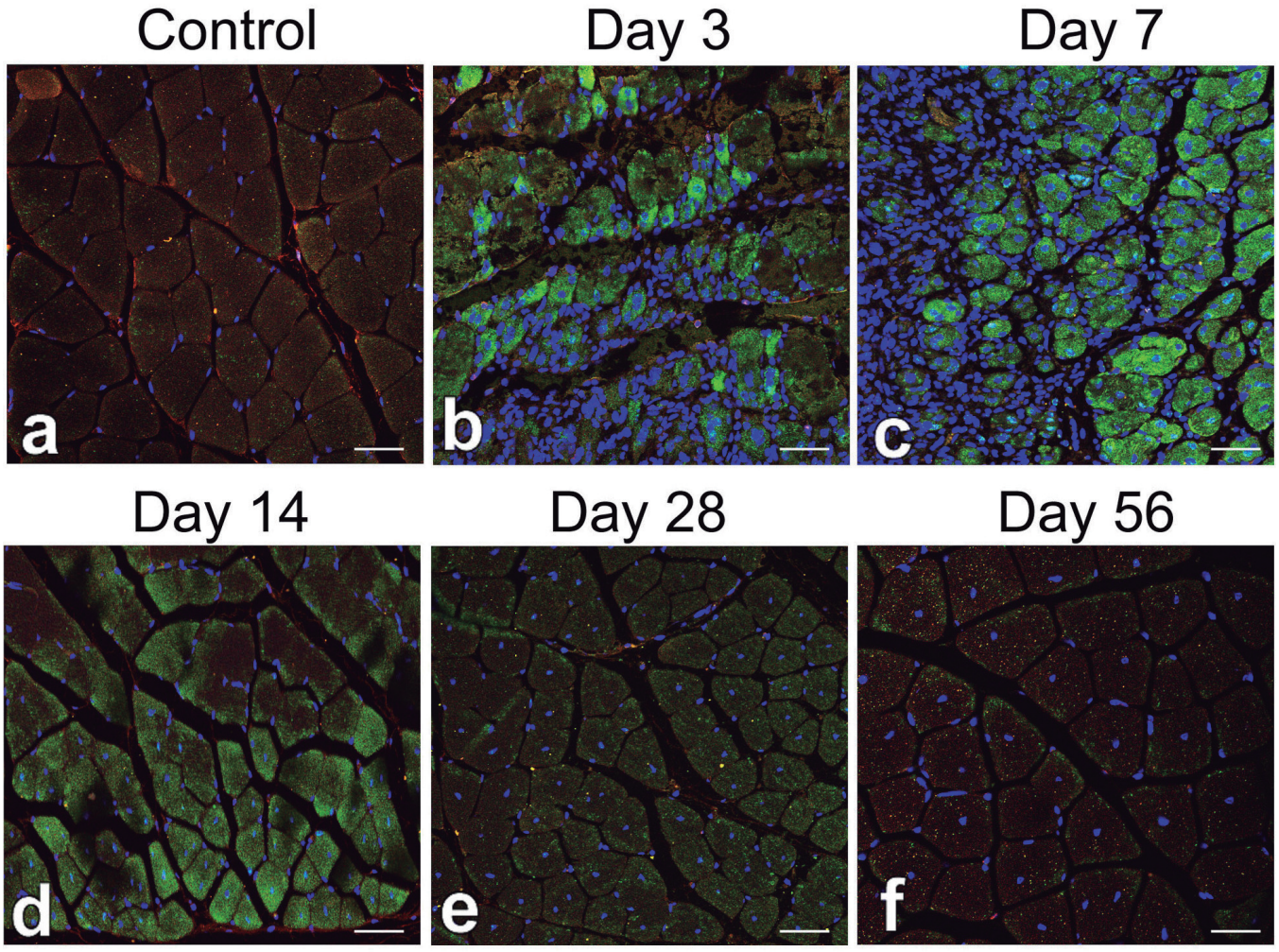

Fig. 3. Immunofluorescence staining for PS (red) and MYH3 in the gastrocnemius muscle 3, 7, 14, 28, and 56 days after CTX injection. Saline was injected into the gastrocnemius of control mice. Nuclei stained by DAPI are in blue. MYH3 was clearly localised in the cytoplasm of regenerated myofibres with internal nuclei at 3, 7, and 14 days post-CTX injection **(b, c, and d)** but was much less in the control myofibres **(a)** and in the regenerated myofibres at 28 and 56 days post-CTX injection **(e, f)**. Bars: 50 μm.

(data not shown).

Because the PS-positive infiltrated cells were identified as macrophages, PS mRNA expression in the macrophages was also analysed using *in situ* hybridisation. The result showed that PS mRNA was clearly expressed in the infiltrating area and that the PS mRNA isoform in these cells (macrophages) was also Pro+0 (Fig.11).

MAP kinase activity in mdx and CTX-treated gastrocnemius muscles

The activation of the MAPK pathway by PS, saposin C, or TX14A has been found for many neuronal- or glial-derived cells, such as PC12, Schwann, and neuroblastoma cells (Campana et al., 1998; Misasi et al., 2001). To determine whether PS is associated with the MAPK pathway in muscle regeneration, we evaluated the expression of p38 MAPK and ERK, and phosphorylated p38 MAPK and ERK in mdx and CTX-treated gastrocnemius muscles by Western blot analysis.

In CTX-treated muscles, phosphorylated p38 MAPK increased from day 3 to day 14, but decreased on day 56 compared with age-matched controls. The phosphorylated ERK decreased on day 7 but increased on day 28 and day 56 (Fig. 12a-c). The total protein expression levels of these two kinases were not affected by CTX.

Our immunoblotting results also revealed a decrease in p38 MAPK phosphorylation without altering total protein levels both in young and old mdx mice compared with the C57BL group (Fig. 12d,e; $p<0.01$). At the same time, a significant increase in phosphorylated ERK1/2 was observed in mdx muscles, particularly at 4 weeks (Fig. 12d,f; $p<0.01$ vs. C57BL group), while the total ERK1/2 protein levels remained unchanged.

Discussion

Prosaposin expression in the regenerated muscles of cardiotoxin-treated mice

As a neurotrophic factor, large amounts of PS exist in skeletal muscle (Sano et al., 1989) and intense PS immunoreactivity is observed in all types of muscle cells, including skeletal, cardiac and smooth muscle. In addition, PS is clearly present in both L6 and chick-embryo myotubes *in vitro* and PS immunoreactivity increases during differentiation *in vitro* (Rende et al., 2001). To date, no report has described PS expression and function during the regeneration of muscle *in vivo*.

In this study, we investigated PS expression in CTX-treated gastrocnemius muscle with immunofluorescence and Western blotting from day 3 to day 56 postinjection.

CTX leads to the depolarization and degradation of the plasma membrane of skeletal muscle cells. Nevertheless, the basal lamina of the muscle fibre remains undamaged, and the regeneration of the damaged muscle fibre takes place within the 'old' basal lamina tube. Myogenic cell differentiation and new myotube formation is observed 3-4 days postinjection. By 14 days postinjection, the overall architecture of the muscle is restored, although most regenerated myofibres are smaller and display central myonuclei (Fig. 1d). The return to a morphologically and histochemically normal mature muscle is seen at 3-4 week postinjection (Charge and Rudnicki, 2004).

MYH3 immunoreactivity was evident in newly regenerated myofibres on days 3, 7, and 14 post-CTX injection (Fig. 3b-d). After muscle architecture was restored, MYH3 immunoreactivity in the regenerated muscle was low after day 28 post-CTX injection (Fig. 3e,f), indicating that the maturation of regenerated myofibres was progressing.

The immunofluorescent results show that PS immunoreactivity was clearly distributed in the peripheral cytoplasm of control muscle and at the late stage in regenerated myofibres (8 weeks postinjection) but was only weakly expressed during the early stage of regenerated muscle (before 4 weeks postinjection (Fig. 1). The expression of PS increased as the maturation of regenerated myofibres progressed, which indicates that PS is involved in the regulation of muscle maturation of regenerated fibres.

PS was also distributed in infiltrating cells (mainly in macrophages, see Fig. 2) in the early stage of

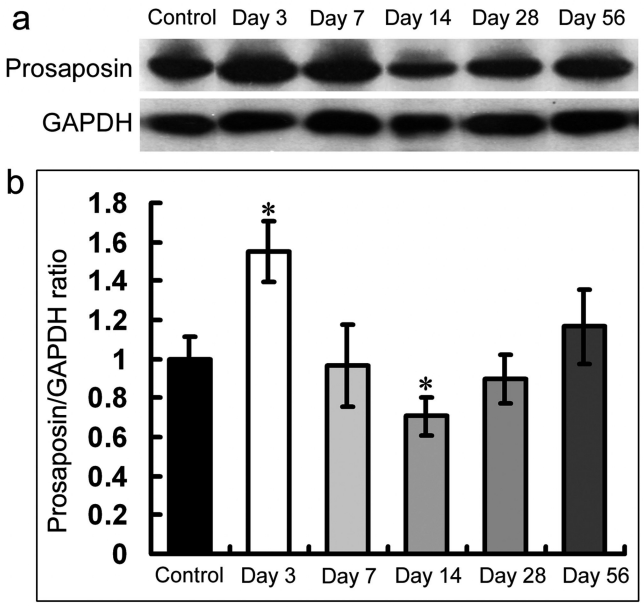

Fig. 4. Western blot analysis of PS in CTX-treated gastrocnemius muscles of C57BL/10 mice. Total protein was extracted from gastrocnemius muscles 3, 7, 14, 28, and 56 days after CTX injection. The amount of GAPDH was measured as an internal control. OD data are expressed as the ratio of PS to GAPDH and were analysed using analysis of variance (ANOVA) followed by least significant difference (LSD) post hoc tests. All values are presented as means±SD. *: $p<0.05$.

regenerated muscles (Fig. 1n,o), as confirmed by Western blotting. The function of macrophages in the regenerated myofibres will be discussed in the following section.

Prosaposin expression in the regenerated muscles of mdx mice

To confirm PS expression in regenerated myofibres,

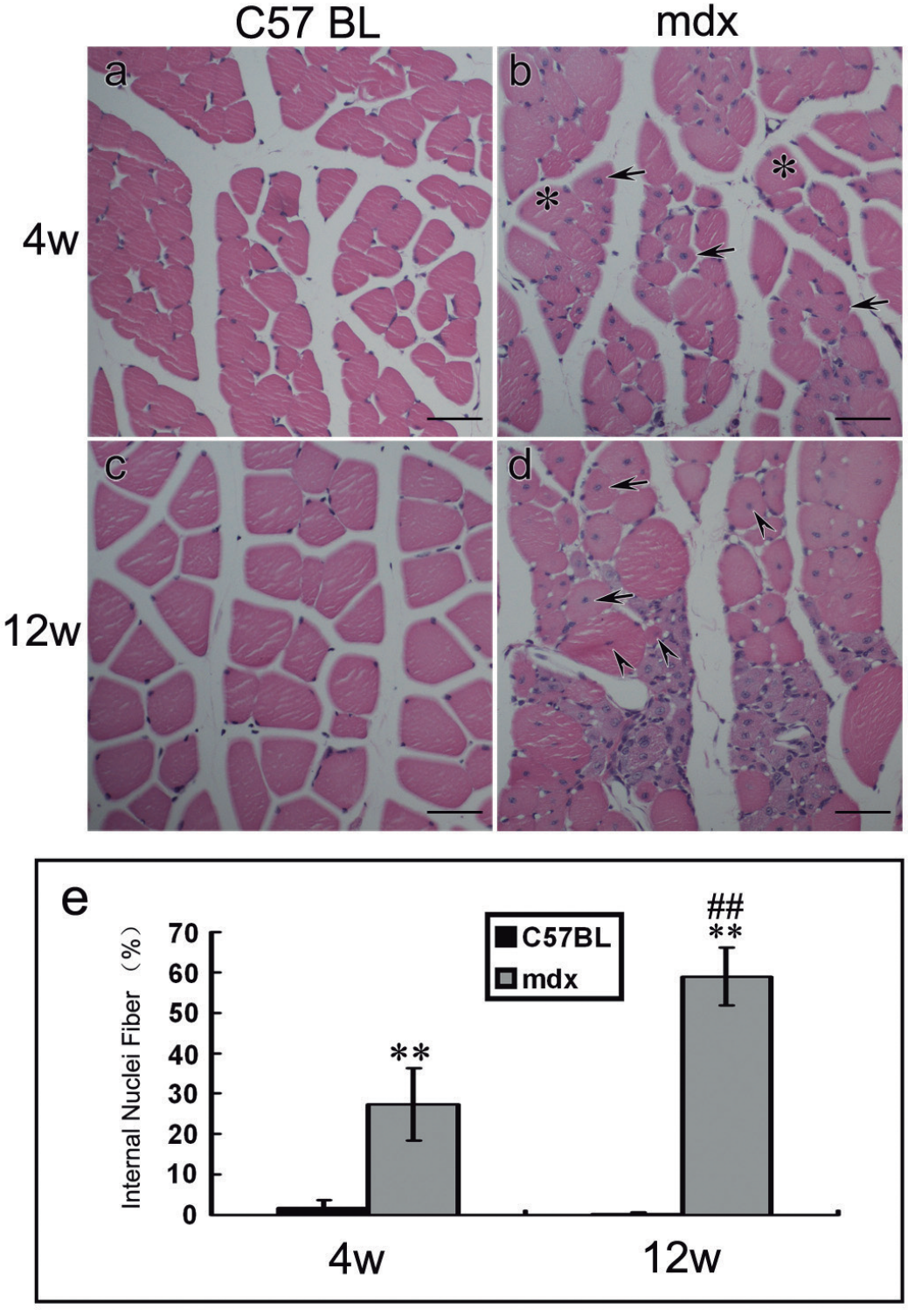

Fig. 5. Transverse sections of the gastrocnemius muscles of control and mdx mice stained with H&E **(a-d).** In the control group, almost no regenerated myofibres with central nuclei were observed at either time point **(a, c).** In mdx mice at 4 weeks of age, many regenerated myofibres with central nuclei (arrows in **b**) co-existed with undamaged myofibres (asterisks in **b**). By 12 weeks of age, most myofibres were replaced by regenerated fibres (arrows in **d**) with variable diameter (arrowheads in **d**). The percentages of regenerated myofibres containing central nuclei were significantly elevated in mdx muscles than those noted in age-matched C57BL/10 mice **: $p<0.01$. Significant differences between 4- and 12-week-old mdx mice are denoted by number signs. ##: $p<0.01$. Bars: 20 μm.

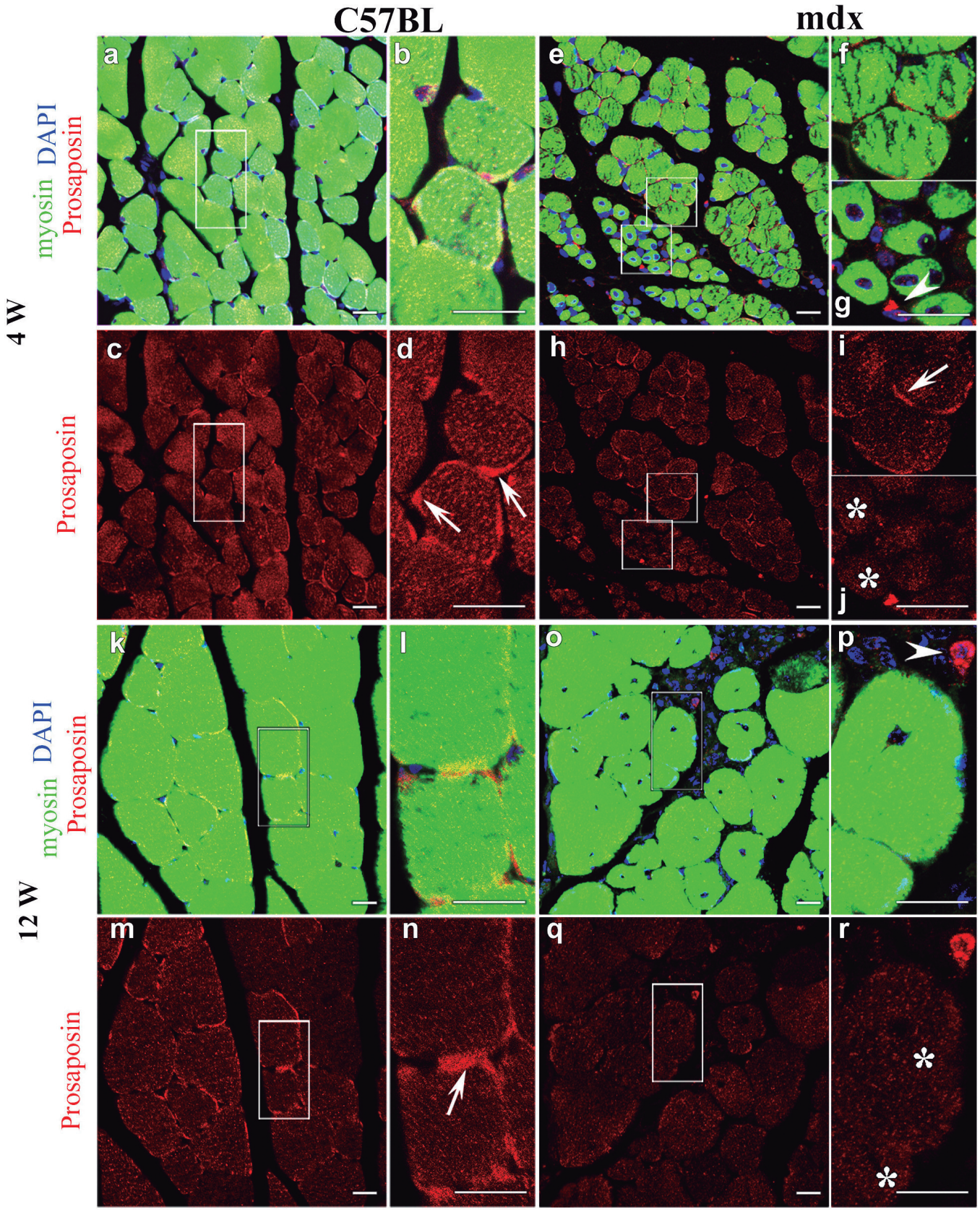

Fig. 6. Immunofluorescence staining for PS (red) and myosin (green) in the gastrocnemius muscle of C57BL/10 (4 weeks, **a-d**; 12 weeks, **k-n**) and mdx mice (4 weeks, **e-j**; 12 weeks, **o-r**) observed using confocal laser microscopy. The boxes in **a**, **e**, **c**, **h**, **k**, **o**, **m**, and **q** were magnified to **b, f+g, d, i+j, l, p, n, and r,** respectively. DAPI stained the nuclei blue. PS was localised in the peripheral cytoplasm of myofibres in control mice (arrows in **d**, **n**) and the undamaged myofibres in mdx mice (arrows in **i**), but was not localised in the regenerated myofibres in mdx mice (asterisks in **j**, **r**). PS was also localised to some non-muscle cells of mdx mice (arrowheads in **g**, **p**) Bars: 20 μm.

we investigated PS expression in the mdx mouse model due to efficient muscle regeneration. Although mdx mice are normal at birth, the lack of dystrophin results in cycles of skeletal muscle necrosis and regeneration. This dystrophic process starts approximately 19-21 days after birth, is very active over the following 5 weeks, and continues at a lower rate throughout the life of the mouse (McGeachie et al., 1993).

Our results also showed that PS immunoreactivity was localised in the peripheral cytoplasm of undamaged myofibres in C57BL and mdx mice, but weakly in the regenerated muscle fibres in mdx mice at both 4 weeks and 12 weeks of age (Fig. 6). PS protein levels decreased in mdx mice, as shown by Western blotting. As expected, the level of PS protein in muscle was lower at 12 weeks than at 4 weeks of age in mdx mice ($p<0.01$) (Fig. 8), because the proportion of regenerated fibres became higher in 12-week-old mice as the disease

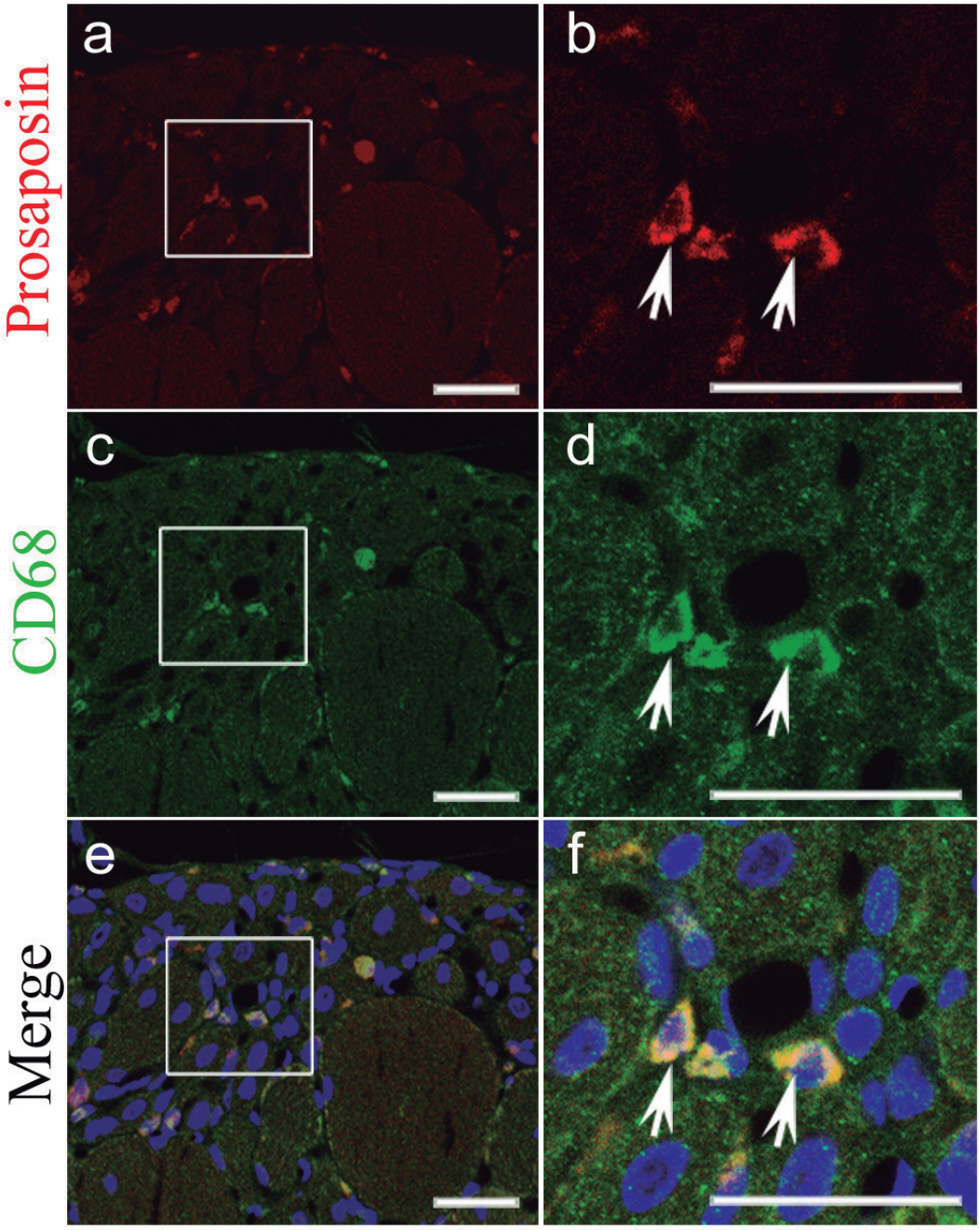

Fig. 7. PS localisation in CD68-positive cells. Immunofluorescent staining of PS (red) with CD68 (green) in the gastrocnemius muscle of 12-week-old mdx mice. Nuclei were stained blue with DAPI. Arrows indicate PS co-localised with CD68 in the cytoplasm of inflammatory cells. CD68 is a marker of mononuclear cells. Bars: 20 μm.

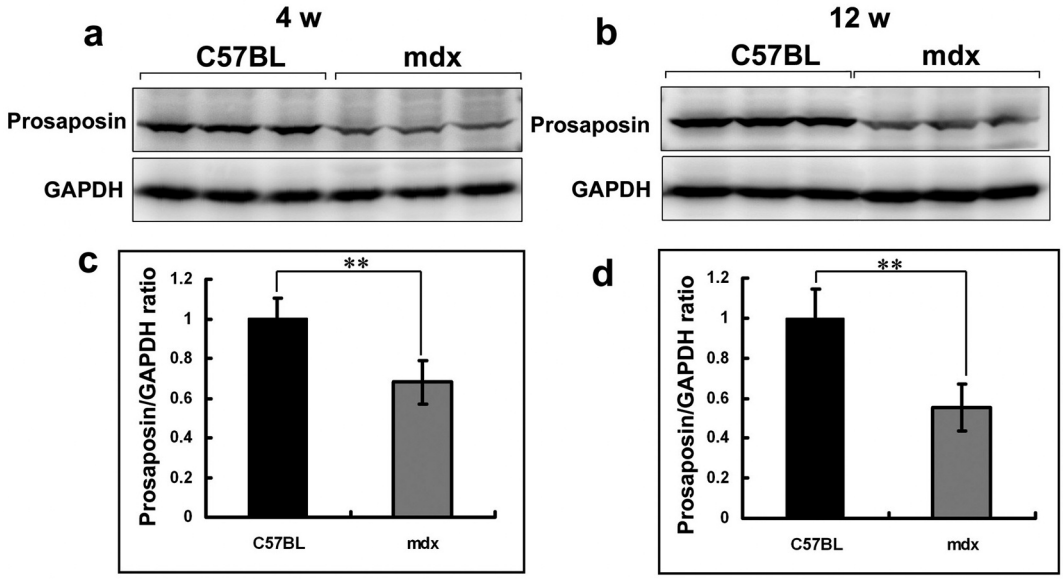

Fig. 8. Expression of PS in the gastrocnemius muscles of C57BL/10 and mdx mice, as assessed by Western blotting (**a, c** for 4 weeks of age; **b, d** for 12 weeks). Representative gels for Western blotting (**a, b**). Relative protein expression following densitometry analysis (standardised to C57BL/10) (**c, d**). GAPDH was used as a control for protein loading. Results were analysed using a Mann-Whitney U-test and presented as a histogram. **: $p<0.01$.

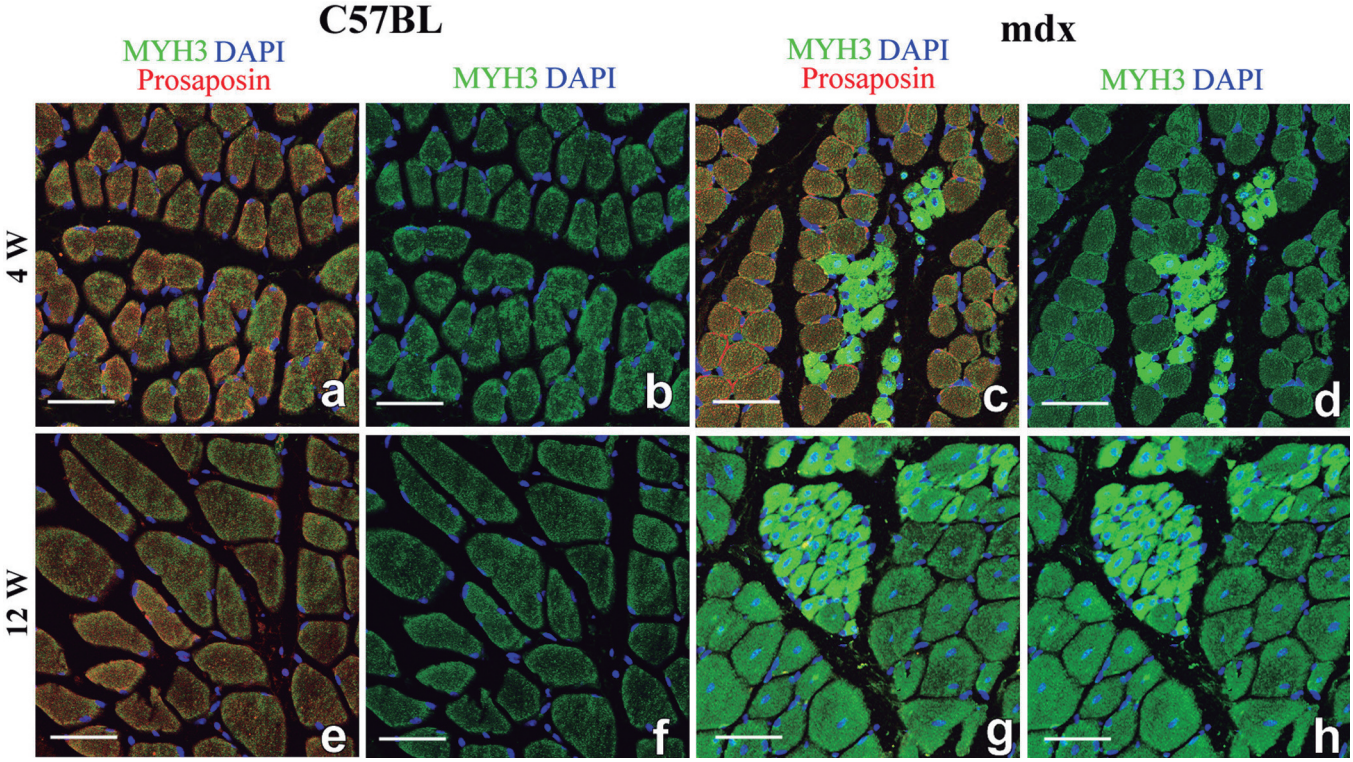

Fig. 9. Immunofluorescence staining for PS (red) and MYH3 (embryonic myosin; green) in the gastrocnemius muscle of C57BL/10 (4 weeks, **a, b**; 12 weeks, **e, f**) and mdx mice (4 weeks, **c, d;** 12 weeks, **g, h**) observed using confocal laser microscopy. DAPI stained the nuclei blue. MYH3 was clearly localised in the cytoplasm of regenerated myofibres in mdx mice at 4 weeks (μ) and regenerated myofibres of small size in mdx mice at 12 weeks. The MYH3 immunoreactivity in the large regenerated myofibres of 12-week mdx mice was less than the small-sized myofibres but still higher than the control (**g, h**). Bars: 50 μm.

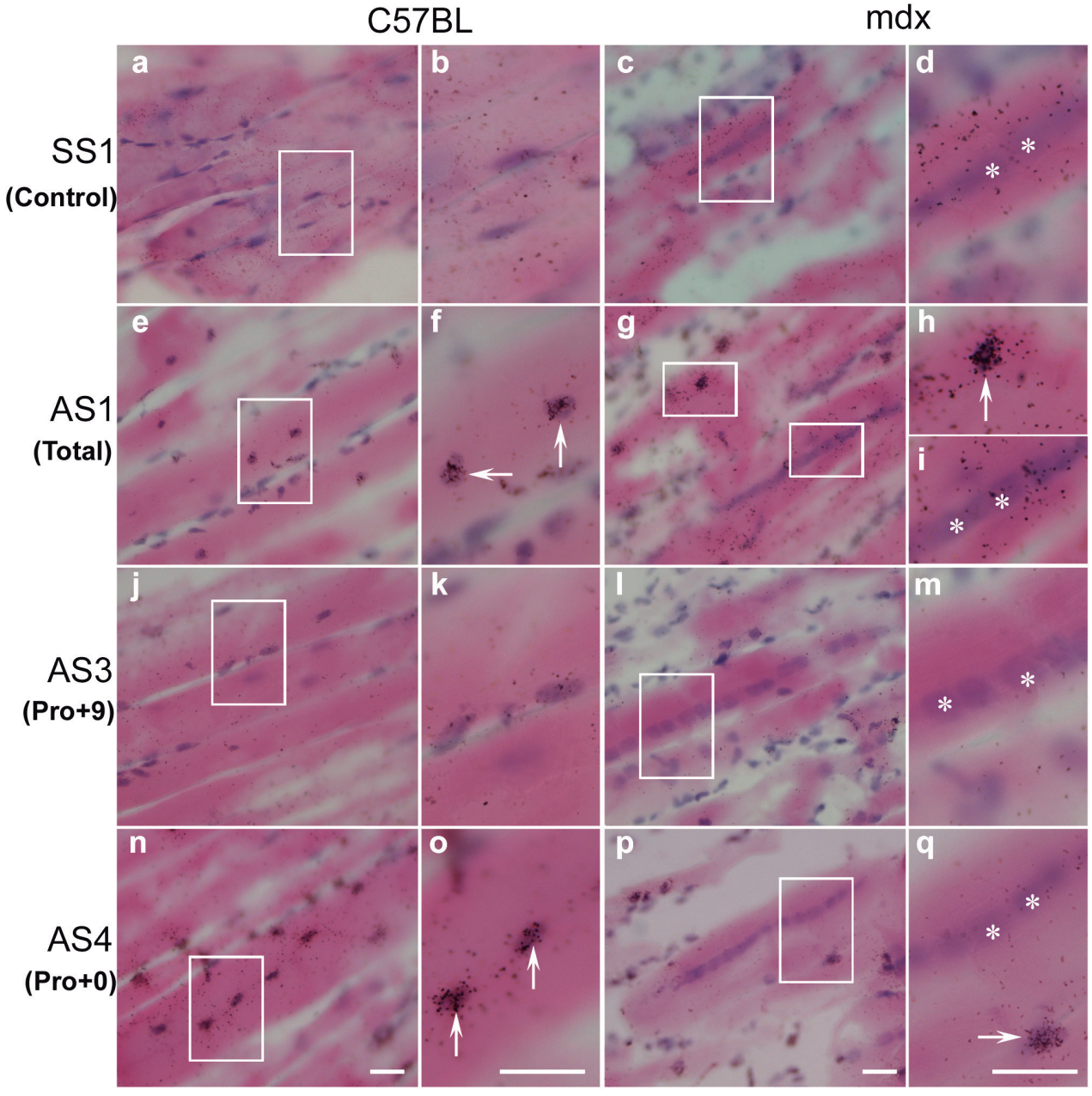

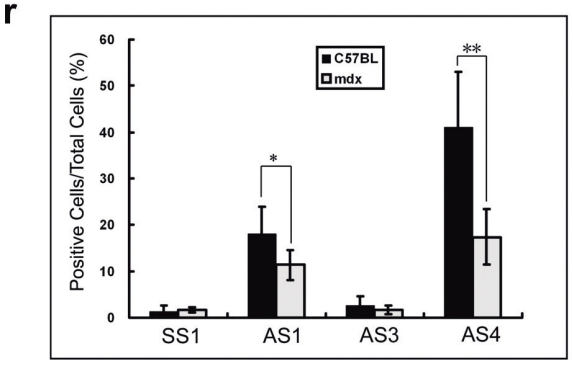

Fig. 10. Expression of PS mRNA in the gastrocnemius muscle of C57BL/10 and mdx mice at 4 weeks. *In situ* hybridisation with [^{35}S]-labelled antisense oligonucleotide probes: AS1 (**e-i)** to detect total mRNA; AS3 (**j-m**) to detect exon 8-containing PS mRNA; and AS4 (**n-q**) to detect exon 8-excluded PS mRNA. One [^{35}S]-labelled sense probe, SS1 (**a-d**), was used as control. The positive nuclei (labelled with concentrated silver grains) can be identified in the myofibres of control mice (arrows in **f, o**) and in undamaged myofibres of mdx mice (arrows in **h, q**), but not in the regenerated myofibres of mdx mice (asterisks in **i, q**) when the AS1 and A4 probes were used. No obvious reactivity exists in AS3 and control (SS1) sections. Results were analysed using analysis of variance (ANOVA) followed by Fischer's least significant different (LSD) post hoc tests and are presented in a histogram. r; *: $p<0.05$, **: $p<0.01$. Bars: 20 μm.

developed (Fig. 5). We also investigated PS expression in masseter, spinalis, and diaphragm muscles using immunofluorescence and Western blotting and found similar results (data not shown). Decreased PS expression in regenerated myofibres was confirmed by *in situ* hybridisation with two different probes (Fig. 10).

Immunofluorescent staining showed that MYH3 immunoreactivity was clearly located in regenerated myofibres in 4-week-old mdx mice muscles and was less so in the control muscles (Fig. 9a-d). In 4-week mdx mice, this was approximately 1 week after necrosis and regeneration had commenced. The distribution of PS and MYH3 in mdx mice muscle was similar to that in the CTX-treated muscle at 1 week postinjection. MYH3 immunoreactivity was also clearly located in regenerated myofibres in 12-week-old mdx mice muscle, which was 9 weeks after the first major bout of regeneration (Fig. 9g,h). Although the centrally nucleated muscle fibres were observed in the CTX-treated muscle at 8 weeks postinjection (Fig. 1r) and in 12-week-old mdx muscles (Fig. 6q), PS was only expressed in the CTX-treated muscle. This may be due to differences in maturation. In the CTX-treated muscle, after muscle architecture was restored, maturation proceeded as MYH3 expression was inhibited after 56 days post-CTX injection. In contrast, the differentiation of regenerated myofibres in mdx mice was delayed even after 12 weeks, as shown by clear MYH3 expression not only in the small myoblasts, but also in the large myotubes with central nuclei (Fig. 9h).

Earnshaw et al. (2002) also showed that the differentiation of regenerated muscle clusters was clearly delayed in mdx muscles because few muscle fibres appeared to be fully differentiated even at 14 weeks of age. Our result is in agreement with Earnshaw's study and indicates that the maturation of regenerated myofibres was clearly delayed in mdx muscles. The reduction of PS in the delayed regenerated myofibres indicates that PS is involved in the regulation of muscle differentiation of regenerated fibres.

Molecular events in the regenerated muscle

Muscle regeneration after injury is similar in *in vitro* and *in vivo* experiments, and the potential role of related growth factors attracts considerable attention (Charge and Rudnicki, 2004) (Fig. 13). The quiescent satellite cells are activated to enter the cell cycle and proliferate, followed by differentiation and fusion of myoblasts (Fig. 13a-c). The regenerated myofibres are morphologically typified by small-calibre, centrally nucleated fibres (Fig. 13d). Finally, repaired or newly formed myofibres develop into mature myofibres (Fig. 13e).

Many growth factors are reported to be involved in the process of muscle regeneration, including fibroblast growth factor (FGF), hepatocyte growth factor (HGF), insulin-like growth factor (IGF), tumour necrosis factor-α (TNF-α), and interleukin-6 (IL-6). *In vitro* and *in vivo* experiments have highlighted the positive role of FGF, HGF, IGF, and IL-6 (Charge and Rudnicki, 2004; Hawke and Garry, 2001). For example, injection of basic FGF (bFGF) in mdx mice appeared to improve satellite cell proliferation and muscle regeneration (Lefaucheur and Sebille, 1995). We also reported that the immature myoblast in mdx mice showed more intense bFGF immunoreactivity as compared with mature muscles. Regenerated immature muscles may stimulate their own regeneration or differentiation with bFGF in a paracrine or autocrine manner (Matsuda et al., 1992). The present study showed that normal myoblasts and myotubes strongly expressed PS mRNA (Fig. 10) and PS protein (Figs. 6, 8).

In the study of the inflammatory cells in relation to muscle regeneration, macrophages have received

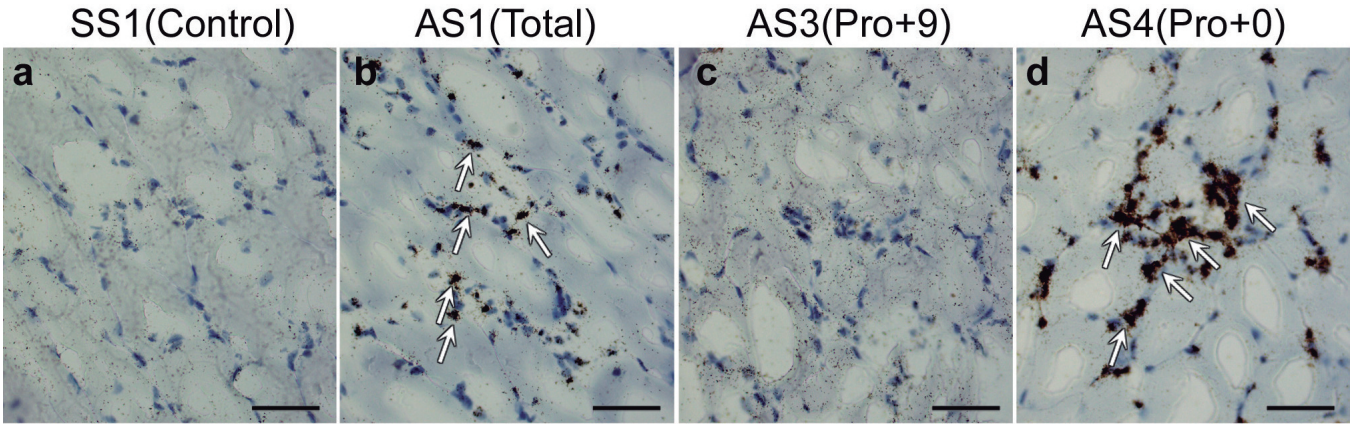

Fig. 11. Expression of PS mRNA in the gastrocnemius muscle of mdx mice at 4 weeks. *In situ* hybridisation with three [^{35}S]-labelled antisense oligonucleotide probes (AS1 to detect total mRNA, AS3 for exon 8-containing PS mRNA, and AS4 for exon 8-excluded PS mRNA) and one [^{35}S]-labelled sense probe (SS1 used as control), all counterstained with haematoxylin. The distribution of the nuclei indicates they are from infiltrating cells **(a-d).**The arrows indicate the positive nuclei that are present in AS1 and AS4 sections (**b, d**) but not in AS3 and control (SS1) sections (**a, c**). Bars: 50 μm.

considerable attention (Villalta et al., 2011). Macrophages promote muscle damage *in vitro and in vivo* by the production of cytotoxic levels of nitric oxide (NO) during the early stage of muscle inflammation. Macrophages are also able to promote muscle growth and repair by producing TNF-α, and the expression of TNF-α during the regenerative process could modulate muscle proliferation and differentiation (Zador et al., 2001). In the present study, macrophage recruitment into injured muscle was shown in both CTX-treated and mdx mice. The protein and mRNA of PS were highly expressed in the macrophages infiltrating the muscles (Figs. 7, 11).

PS mRNA has two main isoforms: with and without exon 8 (Holtschmidt et al., 1991). The PS expressed in both myotubes and macrophages was exon-8 excluded (Figs. 10, 11). It was reported that the PS containing the extra three amino acids was more efficiently secreted from HeLa cells infected with vaccinia virus-derived vectors than was the isoform lacking them (Madar-Shapiro et al., 1999). However, a more recent study strongly indicated that the PS variant containing exon 8 was nonessential for PS secretion and its lysosomal function (Cohen et al., 2005). Therefore, the PS in myotubes and macrophages may be secreted and involved in the regeneration of nearby myofibres. Rende

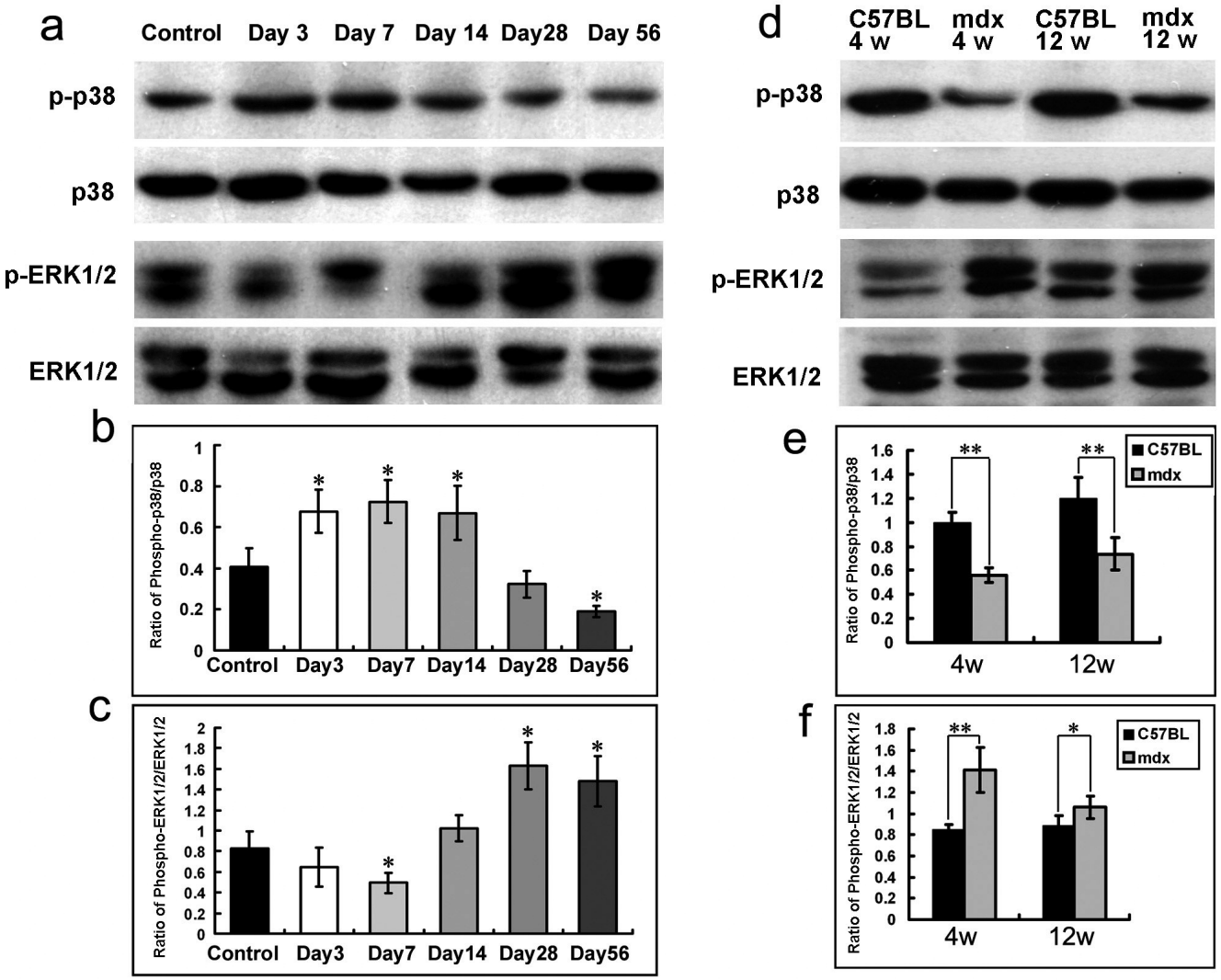

Fig. 12. Expression of MAP kinases in CTX-treated wild-type mice (**a-c**), and non-treated mdx and control mice (**d-f**). **a-c.** Gastrocnemius muscles of C57BL/10 mice were extracted on 3, 7, 14, 28, and 56 days post-CTX injection. **d-f.** The gastrocnemius muscles of young (4 weeks) and adult (12 weeks) mdx mice and age-matched C57BL/10 mice were extracted. Equal amounts of whole cell lysate (30 μg) were subjected to electrophoresis and analysed by Western blotting. Activation of p38 MAPK and ERK1/2 was examined using respective antibodies against phosphorylated and non-phosphorylated p38 MAPK and ERK1/2. OD data are expressed as the ratio of phosphorylated kinases to non-phosphorylated proteins. At least three independent experiments were performed that all showed similar results. All values are means±SD. *: p<0.05, **: p<0.01 compared with the control group.

et al. (2001) showed that the peptide derived from the neurotrophic sequence of PS induced a threefold increase in L6 myoblast fusion during the early stages of differentiation. In the present study, PS secreted by myotubes and macrophages may promote myoblast fusion in an autocrine and/or paracrine manner (Fig. 10). Furthermore, we also showed that PS displayed low expression in the regenerated myofibres at the early stage when induced by CTX and in regenerated myofibres with delayed maturation of mdx mice, whereas PS was clearly expressed in the regenerated myofibres of the late stage in CTX-treated mice and in normal control mice. These results indicate that PS is a regulator of myoblast differentiation and suggest PS involvement in the pathology of mdx mice.

Because the neurotrophic function of PS was associated with the MAPK pathway (Campana et al., 1998), we also investigated ERKs and p38 MAPK activity in the regenerated muscles of CTX-treated and mdx mice. P38 MAPK is recognised as a necessary and sufficient "switch" that turns on the differentiation programme (Cabane et al., 2003; Keren et al., 2006). Inhibition of ERK1/2 activities enhances the activation of p38 MAPK, which results in enhancement of myoblast differentiation, whereas inhibition of p38 MAPK activity enhances ERK1/2 activities, culminating in abrogation of differentiation (Khurana and Dey, 2002). In our study, phosphorylated ERK increased and

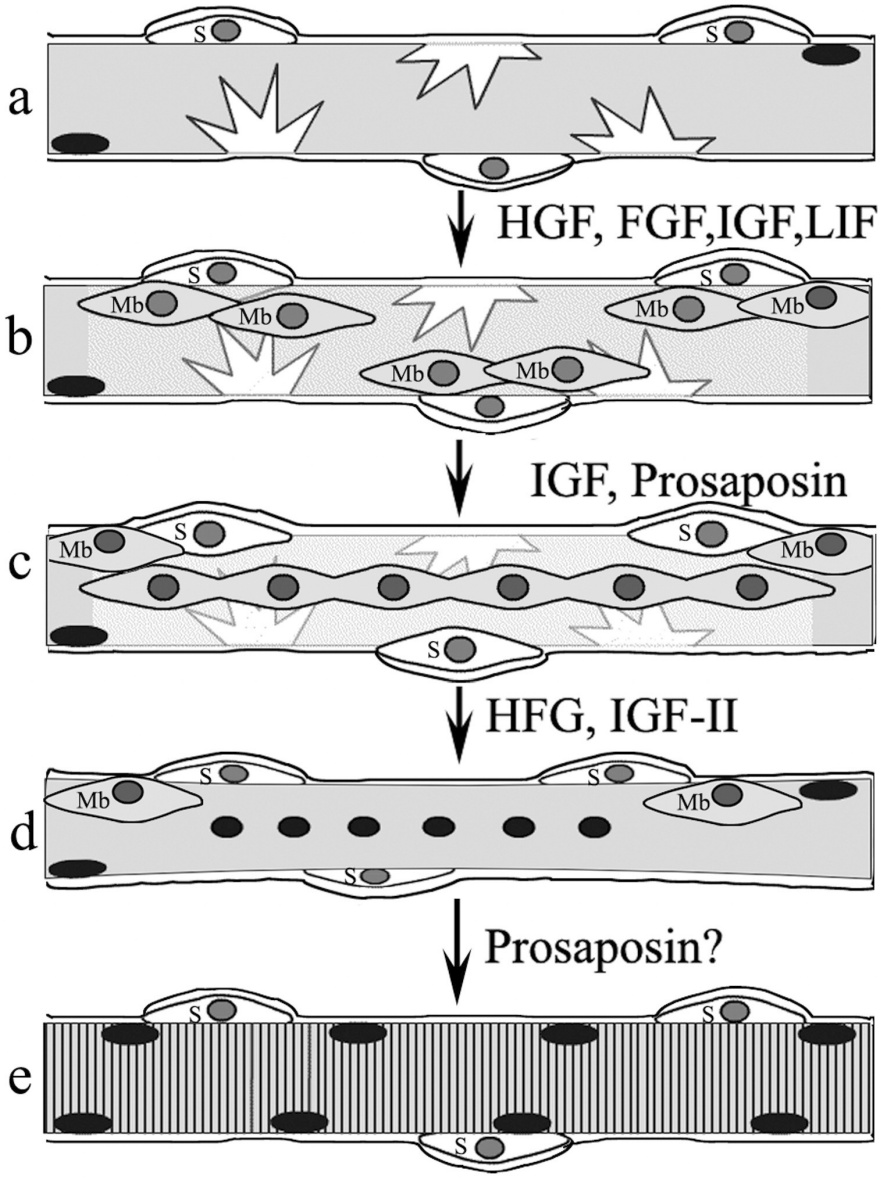

Fig. 13. Schematic representation of molecular events during skeletal muscle regeneration. Following damage to the myofibre **(a)**, quiescent satellite cells were activated to enter the cell cycle and proliferate, allowing for expansion of the myogenic cell population **(b).** The proliferative phase was followed by differentiation and fusion of myoblasts to damaged myofibres for repair or to each other for new myofibre formation **(c)**. The regenerated myofibres were morphologically identified by small-calibre, centrally nucleated fibres **(d)**. Finally, repaired or new myofibres grew to resemble normal myofibres **(e)**. Several growth factors were involved in the course of muscle regeneration (Charge and Rudnicki, 2004). PS has been suggested to increase the ratio of fusion (Rende et al., 2001) and may have a potential role in the growth of regenerated muscle. HGF, hepatocyte growth factor; FGF, fibroblast growth factor; IGF, insulin-like growth factor; IL-6, interleukin-6; LIF, leukaemia inhibitory factor; S, satellite cell; Mb, myoblast cell.

phosphorylated p38 MAPK decreased in the muscles of 4- and 12-week-old mdx mice (Fig. 12d-f), which agrees with the observation of Hnia et al. (2007). Our results also showed that phosphorylated ERKs decreased whereas phosphorylated p38 MAPKs increased in gastrocnemius muscle 3 days after CTX treatment. The inversely synchronous correlation of phosphorylated ERK1/2 with myofibre PS and the synchronous correlation of phosphorylated p38 with myofibre PS indicate that PS inhibits ERK phosphorylation but promotes p38 MAPK phosphorylation. In contrast, several studies demonstrated that exogenous PS induced ERK phosphorylation (Campana et al., 1998; Misasi et al., 2004; Sorice et al., 2008). The explanation of these reported differences may in part lie in the different methods used. All of these experiments were carried out *in vitro* with cultured cells. However, they also indicated that some other factors that could trigger the ERK-signalling pathway are involved in the regeneration and maturation of CTX-treated and dystrophic mdx mouse muscle.

Collectively, our findings show that PS is downregulated in the muscles during early stages of regeneration in CTX-treated mice and mdx mice, and these data indicate that PS is involved in the regulation of muscle differentiation of regenerated fibres *in vivo*. The results of this study suggest that PS may have value as a therapeutic agent for the treatment of DMD or other muscle diseases.

Acknowledgements. This study was supported in part by grants to TS (No. 25450466), SM (Nos. 22591637, 25462295) and NK (No. 24590254) from the Ministry of Education, Culture, Sports, Science and Technology of Japan.

References

Attal P., Lambert F., Marchand-Adam S., Bobin S., Pourny J.C., Chemla D., Lecarpentier Y. and Coirault C. (2000). Severe mechanical dysfunction in pharyngeal muscle from adult mdx mice. Am. J. Respir. Crit. Care Med. 162, 278-281.

Bulfield G., Siller W.G., Wight P.A. and Moore K.J. (1984). X chromosome-linked muscular dystrophy (mdx) in the mouse. Proc. Natl. Acad. Sci. USA 81, 1189-1192.

Cabane C., Englaro W., Yeow K., Ragno M. and Derijard B. (2003). Regulation of C2C12 myogenic terminal differentiation by MKK3/p38alpha pathway. Am. J. Physiol. Cell Physiol. 284, C658-666.

Campana W.M., Hiraiwa M. and O'Brien J.S. (1998). Prosaptide activates the MAPK pathway by a G-protein-dependent mechanism essential for enhanced sulfatide synthesis by Schwann cells. FASEB J. 12, 307-314.

Charge S.B. and Rudnicki M.A. (2004). Cellular and molecular regulation of muscle regeneration. Physiol. Rev. 84, 209-238.

Chen J., Saito S., Kobayashi N., Sato K., Terashita T., Shimokawa T., Mominoki K., Miyawaki K., Sano A. and Matsuda S. (2008). Expression patterns in alternative splicing forms of prosaposin mRNA in the rat facial nerve nucleus after facial nerve transection. Neurosci. Res. 60, 82-94.

Chiou S.H., Raynor R.L., Zheng B., Chambers T.C. and Kuo J.F. (1993). Cobra venom cardiotoxin (cytotoxin) isoforms and neurotoxin: comparative potency of protein kinase C inhibition and cancer cell cytotoxicity and modes of enzyme inhibition. Biochemistry 32, 2062-2067.

Cohen T., Auerbach W., Ravid L., Bodennec J., Fein A., Futerman A.H., Joyner A.L. and Horowitz M. (2005). The exon 8-containing prosaposin gene splice variant is dispensable for mouse development, lysosomal function, and secretion. Mol. Cell. Biol. 25, 2431-2440.

Collard M.W., Sylvester S.R., Tsuruta J.K. and Griswold M.D. (1988). Biosynthesis and molecular cloning of sulfated glycoprotein 1 secreted by rat Sertoli cells: sequence similarity with the 70-kilodalton precursor to sulfatide/GM1 activator. Biochemistry 27, 4557-4564.

Earnshaw J.C., Kyprianou P., Krishan K. and Dhoot G.K. (2002). Differentiation of original and regenerated skeletal muscle fibres in mdx dystrophic muscles. Histochem. Cell Biol. 118, 19-27.

Grounds M.D., White J.D., Rosenthal N. and Bogoyevitch M.A. (2002). The role of stem cells in skeletal and cardiac muscle repair. J. Histochem. Cytochem. 50, 589-610.

Hawke T.J. and Garry D.J. (2001). Myogenic satellite cells: physiology to molecular biology. J. Appl. Physiol. 91, 534-551.

Hineno T., Sano A., Kondoh K., Ueno S., Kakimoto Y. and Yoshida K. (1991). Secretion of sphingolipid hydrolase activator precursor, prosaposin. Biochem. Biophys. Re.s Commun. 176, 668-674.

Hiraiwa M., Taylor E.M., Campana W.M., Darin S.J. and O'Brien J.S. (1997). Cell death prevention, mitogen-activated protein kinase stimulation, and increased sulfatide concentrations in Schwann cells and oligodendrocytes by prosaposin and prosaptides. Proc. Natl. Acad. Sci. USA 94, 4778-4781.

Hiraiwa M., Campana W.M., Mizisin A.P., Mohiuddin L. and O'Brien J.S. (1999). Prosaposin: a myelinotrophic protein that promotes expression of myelin constituents and is secreted after nerve injury. Glia 26, 353-360.

Hiraiwa H., Sawazaki T., Suzuki K., Fujishima-Kanaya N., Toki D., Ito Y., Uenishi H., Hayashi T., Awata T. and Yasue H. (2003). Elucidation of correspondence between swine chromosome 4 and human chromosome 1 by assigning 27 genes to the ImpRH map, and development of microsatellites in the proximity of 14 genes. Cytogenet. Genome Res. 101, 84-89.

Hnia K., Hugon G., Rivier F., Masmoudi A., Mercier J. and Mornet D. (2007). Modulation of p38 mitogen-activated protein kinase cascade and metalloproteinase activity in diaphragm muscle in response to free radical scavenger administration in dystrophin-deficient Mdx mice. Am. J. Pathol. 170, 633-643.

Holtschmidt H., Sandhoff K., Kwon H.Y., Harzer K., Nakano T. and Suzuki K. (1991). Sulfatide activator protein. Alternative splicing that generates three mRNAs and a newly found mutation responsible for a clinical disease. J. Biol. Chem. 266, 7556-7560.

Keren A., Tamir Y. and Bengal E. (2006). The p38 MAPK signaling pathway: a major regulator of skeletal muscle development. Mol. Cell Endocrinol. 252, 224-230.

Khurana A. and Dey C.S. (2002). Subtype specific roles of mitogen activated protein kinases in L6E9 skeletal muscle cell differentiation. Mol. Cell Biochem. 238, 27-39.

Lefaucheur J.P. and Sebille A. (1995). Basic fibroblast growth factor promotes *in vivo* muscle regeneration in murine muscular dystrophy.

Neurosci. Lett. 202, 121-124.

Madar-Shapiro L., Pasmanik-Chor M., Vaccaro A.M., Dinur T., Dagan A., Gatt S. and Horowitz M. (1999). Importance of splicing for prosaposin sorting. Biochem. J. 337 (Pt 3), 433-443.

Matsuda S., Desaki J., Fujita H., Okumura N. and Sakanaka M. (1992). Immuno-electron-microscopic localization of basic fibroblast growth factor in the dystrophic mdx mouse masseter muscle. Cell Tissue Res. 270, 569-576.

McGeachie J.K., Grounds M.D., Partridge T.A. and Morgan J.E. (1993). Age-related changes in replication of myogenic cells in mdx mice: quantitative autoradiographic studies. J. Neurol. Sci. 119, 169-179.

Misasi R., Sorice M., Di Marzio L., Campana W.M., Molinari S., Cifone M.G., Pavan A., Pontieri G.M. and O'Brien J.S. (2001). Prosaposin treatment induces PC12 entry in the S phase of the cell cycle and prevents apoptosis: activation of ERKs and sphingosine kinase. FASEB J. 15, 467-474.

Misasi R., Garofalo T., Di Marzio L., Mattei V., Gizzi C., Hiraiwa M., Pavan A., Grazia Cifone M. and Sorice M. (2004). Prosaposin: a new player in cell death prevention of U937 monocytic cells. Exp. Cell Res. 298, 38-47.

Muller J., Vayssiere N., Royuela M., Leger M.E., Muller A., Bacou F., Pons F., Hugon G. and Mornet D. (2001). Comparative evolution of muscular dystrophy in diaphragm, gastrocnemius and masseter muscles from old male mdx mice. J. Muscle Res. Cell Motil. 22, 133-139.

O'Brien J.S., Carson G.S., Seo H.C., Hiraiwa M. and Kishimoto Y. (1994). Identification of prosaposin as a neurotrophic factor. Proc. Natl. Acad. Sci. USA 91, 9593-9596.

Rende M., Brizi E., Donato R., Provenzano C., Bruno R., Mizisin A.P., Garrett R.S., Calcutt N.A., Campana W.M. and O'Brien J.S. (2001). Prosaposin is immunolocalized to muscle and prosaptides promote myoblast fusion and attenuate loss of muscle mass after nerve injury. Muscle Nerve 24, 799-808.

Sandhoff K. and Kolter T. (2003). Biosynthesis and degradation of mammalian glycosphingolipids. Philos. Trans. R. Soc. Lond. B Biol. Sci. 358, 847-861.

Sano A., Hineno T., Mizuno T., Kondoh K., Ueno S., Kakimoto Y. and Inui K. (1989). Sphingolipid hydrolase activator proteins and their precursors. Biochem. Biophys. Res. Commun. 165, 1191-1197.

Sano A., Matsuda S., Wen T.C., Kotani Y., Kondoh K., Ueno S., Kakimoto Y., Yoshimura H. and Sakanaka M. (1994). Protection by prosaposin against ischemia-induced learning disability and neuronal loss. Biochem. Biophys. Res. Commun. 204, 994-1000.

Simerly R.B., Chang C., Muramatsu M. and Swanson L.W. (1990). Distribution of androgen and estrogen receptor mRNA-containing cells in the rat brain: an *in situ* hybridization study. J. Comp. Neurol. 294, 76-95.

Sorice M., Molinari S., Di Marzio L., Mattei V., Tasciotti V., Ciarlo L., Hiraiwa M., Garofalo T. and Misasi R. (2008). Neurotrophic signalling pathway triggered by prosaposin in PC12 cells occurs through lipid rafts. FEBS J. 275, 4903-4912.

Tanabe Y., Esaki K. and Nomura T. (1986). Skeletal muscle pathology in X chromosome-linked muscular dystrophy (mdx) mouse. Acta Neuropathol. 69, 91-95.

Torres L.F. and Duchen L.W. (1987). The mutant mdx: inherited myopathy in the mouse. Morphological studies of nerves, muscles and end-plates. Brain 110 (Pt 2), 269-299.

Unuma K., Chen J., Saito S., Kobayashi N., Sato K., Saito K., Wakisaka H., Mominoki K., Sano A. and Matsuda S. (2005). Changes in expression of prosaposin in the rat facial nerve nucleus after facial nerve transection. Neurosci. Res. 52, 220-227.

Villalta S.A., Rinaldi C., Deng B., Liu G., Fedor B. and Tidball J.G. (2011). Interleukin-10 reduces the pathology of mdx muscular dystrophy by deactivating M1 macrophages and modulating macrophage phenotype. Hum. Mol. Genet. 20, 790-805.

Whalen R.G., Harris J.B., Butler-Browne G.S. and Sesodia S. (1990). Expression of myosin isoforms during notexin-induced regeneration of rat soleus muscles. Dev. Biol. 141, 24-40.

Xue B., Chen J., Gao H., Saito S., Kobayashi N., Shimokawa T., Nabeka H., Sano A. and Matsuda S. (2011). Chronological changes in prosaposin in the developing rat brain. Neurosci. Res. 71, 22-34.

Zador E., Mendler L., Takacs V., de Bleecker J. and Wuytack F. (2001). Regenerating soleus and extensor digitorum longus muscles of the rat show elevated levels of TNF-alpha and its receptors, TNFR-60 and TNFR-80. Muscle Nerve 24, 1058-1067.

Accepted January 8, 2013